Dyes and Pigments 111 (2014) 176–184

Contents lists available at ScienceDirect

Dyes and Pigments

journal homepage: www.elsevier.com/locate/dyepig

Isomorphous and isostructural lanthanide coordination polymers based on 2-(4-chlorobenzoyl)benzoic acid: Synthesis, structure, characterization, and luminescent properties

Lirong Yang*, Liu Liu, Lanzhi Wu, Zhenhuan Xu, Lice Wang

Henan Key Laboratory of Polyoxometalate, Institute of Molecule and Crystal Engineering, College of Chemistry and Chemical Engineering, Henan University, Jinming Street, Kaifeng 475004, PR China

ARTICLE INFO

Article history:
Received 7 March 2014
Received in revised form
7 May 2014
Accepted 9 June 2014
Available online 18 June 2014

Keywords:
Coordination polymers
Luminescent properties
Hydrothermal synthesis
Double-stranded helix
Lanthanide-organic frameworks
Self-assembly

ABSTRACT

Self-assembly of a flexible ligand Hcbba (2-(4-chlorobenzoyl)benzoic acid) and lanthanide salts yield a series of three-dimensional (3D) coordination polymers under hydrothermal conditions, namely, $[Ln(cbba)_3H_2O]_\infty$ (Ln = La(**I**), Pr(**II**), and Nd(**III**)). Their structures were determined by single-crystal X-ray diffraction analyses and characterized by elemental analyses and infrared spectroscopy, which verified that they are isomorphous and isostructural. Findings indicate that the subunit of cavate cages ($Ln_2O_2(OCO)_2$) are observed in **I**–**III**, which are connected into a one-dimensional (1D) chain through $cbba^-$ anions in μ_2-η^1:η^1 fashion and further assembled into 3D architecture *via* C–H···π and C–H···Cl interactions between the neighboring parallel 1D chains. **I**–**III** feature that the double-stranded helix entangled by one left- and one right-handed helical chain coaxially along *c axis* in each 1D infinite chain. Luminescent properties reveal that **II** and **III** may be potential ion-selective luminescent probes for Hg^{2+} and Ag^+, respectively.

1. Introduction

Lanthanide-organic frameworks (LnOFs) have evoked great interest not only the combination of organic and inorganic fragments that can generate a large amount of novel topological structures but also allow that rational design strategies for constructing porous materials with high surface areas, predictable structures, tunable pore sizes and may find potentially industrial applications in gas storage and separation, adsorption catalysis, ion exchange, guest exchange, molecular magnetism, molecular recognition, nonlinear optics and luminescent, etc [1–9]. Additionally, lanthanide ions own larger radius and higher affinity for hard donor centers and ligands with oxygen or hybrid oxygen–nitrogen atoms, which are in favor of the construction of coordination polymers [10–15]. What's more, lanthanide ions with special luminescent resulting from 4f electrons, which illustrated the coordination polymers are intriguing and remarkably suitable for the development of optical devices as well as probes for chemical species [16–20]. Specifically, the conformational freedom nature of the flexible linker Hcbba exhibits several interesting characteristics which may provide more possibility for the construction of novel structures and microporous MOFs: (a) carboxyl and carbonyl may potentially provide various coordination modes and favor the construction of multi-dimensional MOFs. (b) halogen (Cl) atoms may function as electron donor to form hydrogen bonds. (c) specific spatial structure of two benzenes benefit the construction of C–H···π and π···π interactions.

Up to now, only several transition metal coordination polymers based on 2-(4-chlorobenzoyl)benzoic acid has been reported. Following our ongoing efforts towards the synthesis and isolation of lanthanide-containing coordination polymers [21–24]. In this work, we describe the synthesis, structures, and luminescent properties of three 3D coordination polymers obtained from the self-assembly of flexible bridging ligands 2-(4-chlorobenzoyl)benzoic acid and Ln(III) ions, which are formulated as $[La(cbba)_3H_2O]$, $[Pr(cbba)_3H_2O]_\infty$, and $[Nd(cbba)_3H_2O]_\infty$.

2. Experimental section

2.1. Materials and physical measurements

All chemicals were commercially purchased and used without further purification. Elemental analyses (C, H, and N) were performed with a Perkin–Elmer 240 CHN Elemental Analyzer. IR

* Corresponding author.
E-mail address: lirongyang@163.com (L. Yang).

http://dx.doi.org/10.1016/j.dyepig.2014.06.010
0143-7208/

spectra in the range of 400–4000 cm^{-1} were recorded with an AVATAR 360 FT-IR spectrometer (KBr pellets were used). The crystal structure was determined with a Bruker Smart CCD X-ray single-crystal diffractometer. TG analysis was conducted with a Perkin–Elmer TGA7 instrument in flowing N_2 at a heating rate of 10 °C min^{-1}. Excitation and emission spectra were obtained with an F-7000 FL spectrofluorometer at room temperature.

2.2. Synthesis of the coordination polymers *I–III*

$[La(cbba)_3H_2O]_\infty$ (I) was synthesized from the reaction mixture of 2-(4-Chlorobenzoyl)benzoic acid and lanthanum chloride at a molar ratio of 1:1 (0.1 mmol:0.1 mmol) in 10 mL distilled water. The resultant mixture was homogenized by stirring for 30 min at ambient temperature and then transferred into 20 mL Teflon-lined stainless steel autoclave under autogenous pressure at 160 °C for 3 days and then cooled to room temperature at a rate of 5 °C/h. After filtration, the product was washed with distilled water and then dried to afford colorless block-shaped crystals suitable for X-ray diffraction analysis. Elemental analysis calculated (mass fraction, the same hereafter, %) for $C_{42}H_{26}O_{10}Cl_3La$ (935.91): C, 53.64; H, 2.73. Found: C, 53.90; H, 2.80. IR data (KBr pellet, cm^{-1}): 3590(w), 3460(br), 3061(w), 2355(w), 1665(s), 1615(s), 1587(s), 1565(s), 1537(m), 1484(m), 1444(m), 1401(s), 1289(w), 1254(w), 1149(w), 1093(s), 1015(m), 933(s), 887(w), 843(m), 770(w), 748(s), 715(w), 691(w), 677(w), 653(w), 591(w), 561(w), 532(w), 481(w), 426(w).

$[Pr(cbba)_3H_2O]_\infty$ (II) was synthesized by identical experimental procedures to that of **I** except that lanthanum chloride was replaced by praseodymium nitrate. After filtration, the product was washed with distilled water and then dried and primrose transparent crystals suitable for X-ray diffraction analysis were finally isolated. Elemental analysis calculated (%) for $C_{42}H_{26}O_{10}Cl_3Pr$ (937.91): C, 53.99; H, 2.50. Found: C, 53.78; H, 2.79. IR data (KBr pellet, cm^{-1}): 3433(br), 2926(w), 2367(w), 2346(w),1664(m), 1614(s), 1586(s), 1560(w), 1483(w), 1444(w), 1401(s), 1289(w), 1251(w), 1092(w), 1014(w), 964(w), 933(m), 887(w), 842(w), 772(w), 748(m), 716(w), 677(w), 652(w), 531(w), 483(w), 421(w).

$[Nd(cbba)_3H_2O]_\infty$ (III) was synthesized by identical experimental procedures to that of **I** except that lanthanum chloride was replaced by neodymium nitrate. After filtration, the product was washed with distilled water and then dried and purplish transparent crystals suitable for X-ray diffraction analysis were finally isolated. Elemental analysis calculated (%) for $C_{42}H_{26}O_{10}Cl_3Nd$ (941.25): C, 53.88; H, 2.61. Found: C, 53.59; H, 2.78. IR data (KBr pellet, cm^{-1}): 3429(br), 2927(w), 2377(w), 2345(w),1661(m), 1617(s), 1587(s), 1560(w), 1484(w), 1443(w), 1401(s), 1276(w), 1151(w), 1091(w), 1014(w), 965(w), 933(m), 844(w), 772(w), 749(m), 716(w), 677(w), 652(w), 531(w), 439(w), 420(w).

2.3. Crystallographic data collection and refinement

Single-crystal diffraction data **I–III** were collected Suitable single crystals of the coordination polymers on a Bruker Smart CCD X-ray single-crystal diffractometer with graphite monochromated MoKα-radiation (λ = 0.71073 Å) at 296(2) K. All independent reflections were collected in a range of 1.50–25.00° for **I**, 1.49 to 25.00° for **II**, and 2.15 to 25.00° for **III** (determined in the subsequent refinement). Multi-scan empirical absorption corrections were applied to the data using the SADABS. The crystal structure was solved by direct methods and Fourier synthesis. Positional and thermal parameters were refined by the full-matrix least-squares method on F^2 using the SHELXTL software package. The final least-square cycle of refinement gave, $R_1 = 0.0399$, $wR_2 = 0.0803$ for **I**, $R_1 = 0.0636$, $wR_2 = 0.0870$ for **II**, $R_1 = 0.0273$, and $wR_2 = 0.0600$ for **III**. The weighting scheme, $w = 1/[\sigma^2(F_0^2) + (0.0316P)^2 + 0.17.99P]$ for **I**, $w = 1/[\sigma^2(F_0^2) + (0.0459P)^2 + 6048P]$ for **II**, and $w = 1/[\sigma^2(F_0^2) + (0.0278P)^2 + 2.62P]$ for **III**, Where $P = (F_0^2+2F_c^2)/3$. A summary of the key crystallographic information is given in Table 1. Selected bond lengths, bond angles and the parameters of hydrogen bonds for the coordination polymers **I–III** are listed in Table 2 and Table 3, respectively.Table 4.

3. Results and discussion

3.1. The IR spectra of the coordination polymers

Coordination polymers **I–III** are insoluble in common solvents such as CH_3COCH_3, CH_3CH_2OH, CH_3OH, and $CH_3CH_2OCH_2CH_3$, but they are slight soluble in DMSO and DMF. The structures of the coordination polymers are identified by satisfactory elemental analysis as well as FT-IR and X-ray analyses. The FT-IR spectra of the six as-synthesized coordination polymers are similar. The strong and broad absorption bands in the ranges of 3460–3329 cm^{-1} in **I–III** are assigned to the stretching vibrations of ν(O–H) in water molecules in coordination [25–27]. The sharp peaks of δ_{O-C-O} vibration in plane emerge in the range of 748–653 cm^{-1}.The features present in the range of 591 cm^{-1} can be ascribed to the bend vibrations of ν(Ar–CO–Ar) in $cbba^-$ ligands. Another features in the region of 1665–1536 cm^{-1} and 1484–1401 cm^{-1} may be ascribed to the asymmetric (COO^-) and symmetric (COO^-) stretching of carboxyl groups of $cbba^-$ ligands in **I–III**. The values of $\Delta[\nu_{as} - \nu_s]$ are about 264–260 cm^{-1}, which indicate that the carboxyl groups are coordinated with the metal ions *via* both bidentate-chelating

Table 1
Summary of crystallographic data for coordination polymers **I–III**.

Data	I	II	III
Empirical formula	$C_{42}H_{26}Cl_3O_{10}La$	$C_{42}H_{26}Cl_3O_{10}Pr$	$C_{42}H_{26}Cl_3O_{10}Nd$
Formula weight	935.89	937.89	941.22
Temperature/K	296(2)	296(2)	296(2)
Wavelength/Å	0.71073	0.71073	0.71073
Crystal system	Monoclinic	Monoclinic	Monoclinic
space group	*C2/c*	*C2/c*	*C2/c*
a/Å	28.5420(16)	28.561(2)	28.5550(19)
b/Å	10.1480(6)	10.1580(8)	10.0900(7)
c/Å	28.2810(17)	28.301(2)	28.2580(19)
α/(°)	90	90	90
β/(°)	106.2490(11)	106.2330(14)	106.4270(12)
γ/(°)	90	90	90
Z	8	8	8
Density (calculated)	1.581 Mg/m^3	1.580 Mg/m^3	1.601 Mg/m^3
F(000)	3728	3744	3752
Crystal size/mm^3	0.23 × 0.20 × 0.18	0.20 × 0.19 × 0.17	0.21 × 0.20 × 0.17
θ for data collection/(°)	1.500 to 24.999	1.485 to 25.000	2.151 to 24.999
Limiting indices	$-29 \le h \le 33$ $-12 \le k \le 11$ $-33 \le l \le 33$	$-32 \le h \le 33$ $-12 \le k \le 11$ $-31 \le l \le 33$	$-31 \le h \le 33$ $-11 \le k \le 11$ $-31 \le l \le 33$
Reflns collected/ unique	19,612/6902 [$R_{(int)} = 0.0552$]	19,666/6925 [$R_{(int)} = 0.0413$]	19,490/6860 [$R_{(int)} = 0.0332$]
Refinement method	Full-matrix least-squares on F^2		
Data/restraints/ parameters	6902/0/505	6925/0/505	6860/0/505
Goodness-of-fit on F^2	1.041	1.028	1.034
Volume/$Å^3$	7864.2(8)	7883.4(11)	7809.4(9)
Final *R* indices [$I > 2\sigma(I)$]	$R_1 = 0.0399$, $wR_2 = 0.0803$	$R_1 = 0.0636$, $wR_2 = 0.0870$	$R_1 = 0.0273$, $wR_2 = 0.0600$
R indices (all data)	$R_1 = 0.0656$, $wR_2 = 0.0979$	$R_1 = 0.0525$, $wR_2 = 0.0934$	$R_1 = 0.0369$, $wR_2 = 0.0634$
ρ_{min} and ρ_{max}/ ($e \cdot Å^{-3}$)	0.553 and −0.585	0.629 and −0.431	0.515 and −0.419

Table 2
Selected bond lengths (Å) and bond angles (°)for the coordination polymers **I**–**III**.

I					
La1–O9	2.426(3)	La1–O2	2.558(3)	La1–O3	2.527(3)
La1–O6	2.465(3)	La1–O1	2.562(3)	La1–O5	2.534(3)
La1–O8	2.471(3)	La1–O1W	2.660(4)	La1–O6a	2.872(3)
II					
Pr1–O6	2.428(3)	Pr1–O2	2.563(3)	Pr1–O3	2.525(3)
Pr1–O9	2.469(3)	Pr1–O1	2.571(3)	Pr1–O8	2.539(3)
Pr1–O5	2.470(3)	Pr1–O1W	2.662(3)	Pr1–O9a	2.867(3)
III					
Nd1–O2	2.3709(14)	Nd1–O7	2.5127(14)	Nd1–O9	2.4618(16)
Nd1–O6	2.4034(13)	Nd1–O8	2.5133(14)	Nd1–O5	2.4741(14)
Nd1–O3	2.4175(13)	Nd1–O1W	2.6099(14)	Nd1–O6a	2.8733(14)
I					
O9–La1–O6	73.96(11)	O8–La1–O1	140.44(11)	O8–La1–O2	126.31(11)
O9–La1–O8	132.25(11)	O3–La1–O1	87.82(12)	O3–La1–O2	51.16(11)
O6–La1–O8	73.35(11)	O5–La1–O1	68.64(11)	O5–La1–O2	144.40(11)
O9–La1–O3	130.41(12)	O2–La1–O1	77.90(11)	O9–La1–O1	77.67(11)
O6–La1–O3	96.74(12)	O9–La1–O1W	141.36(12)	O6–La1–O1	146.20(11)
O8–La1–O3	87.28(12)	O6–La1–O1W	142.33(11)	O1–La1–O6a	109.32(10)
O9–La1–O5	81.91(12)	O8–La1–O1W	70.83(11)	O6–La1–O6a	76.20(11)
O6–La1–O5	123.86(11)	O3–La1–O1W	70.48(12)	O8–La1–O6a	71.53(11)
O8–La1–O5	88.41(11)	O5–La1–O1W	66.58(11)	O3–La1–O6a	158.76(11)
O3–La1–O5	135.78(12)	O2–La1–O1W	113.65(12)	O5–La1–O6a	47.69(10)
O9–La1–O2	79.36(11)	O1–La1–O1W	70.54(11)	O2–La1–O6a	142.94(11)
O6–La1–O2	79.14(12)	O9–La1–O6a	67.53(11)	O1W–La1–O6a	102.73(11)
II					
O6–Pr1–O9	73.94(9)	O3–Pr1–O1	87.40(10)	O5–Pr1–O2	126.81(9)
O6–Pr1–O5	132.13(9)	O8–Pr1–O1	68.93(9)	O3–Pr1–O2	51.00(9)
O9–Pr1–O5	73.43(9)	O2–Pr1–O1	77.44(9)	O8–Pr1–O2	144.23(9)
O6–Pr1–O3	130.30(10)	O6–Pr1–O1W	141.10(10)	O6–Pr1–O1	77.56(9)
O9–Pr1–O3	97.19(10)	O9–Pr1–O1W	142.19(9)	O9–Pr1–O1	146.09(9)
O5–Pr1–O3	87.83(9)	O5–Pr1–O1W	70.39(9)	O5–Pr1–O1	140.46(9)
O6–Pr1–O8	81.74(10)	O1W–Pr1–O9a	101.99(9)	O9–Pr1–O9a	76.06(9)
O9–Pr1–O8	123.48(9)	O3–Pr1–O1W	71.06(10)	O5–Pr1–O9a	71.34(9)
O5–Pr1–O8	88.07(9)	O8–Pr1–O1W	66.14(9)	O3–Pr1–O9a	159.13(9)
O3–Pr1–O8	135.79(10)	O2–Pr1–O1W	114.19(10)	O8–Pr1–O9a	47.45(8)
O6–Pr1–O2	79.42(10)	O1–Pr1–O1W	70.94(9)	O2–Pr1–O9a	143.09(9)
O9–Pr1–O2	79.60(9)	O6–Pr1–O9a	67.46(9)	O1–Pr1–O9a	109.35(8)
III					
O2–Nd1–O6	74.84(5)	O5–Nd1–O8	143.38(5)	O3–Nd1–O7	139.82(4)
O2–Nd1–O3	132.45(4)	O7–Nd1–O8	76.33(5)	O9–Nd1–O7	87.37(5)
O6–Nd1–O3	73.64(5)	O2–Nd1–O1W	141.28(5)	O5–Nd1–O7	69.67(5)
O2–Nd1–O9	131.05(5)	O6–Nd1–O1W	141.83(5)	O2–Nd1–O8	78.72(5)
O6–Nd1–O9	95.65(5)	O3–Nd1–O1W	70.48(5)	O6–Nd1–O8	79.29(5)
O3–Nd1–O9	86.82(5)	O9–Nd1–O1W	70.00(5)	O3–Nd1–O8	127.90(5)
O2–Nd1–O5	81.34(5)	O5–Nd1–O1W	67.32(5)	O9–Nd1–O6a	158.22(5)
O6–Nd1–O5	124.19(5)	O7–Nd1–O1W	70.18(4)	O5–Nd1–O6a	47.81(4)
O3–Nd1–O5	87.91(5)	O8–Nd1–O1W	113.45(5)	O7–Nd1–O6a	110.56(4)
O9–Nd1–O5	136.23(5)	O2–Nd1–O6a	67.05(4)	O8–Nd1–O6a	142.02(4)
O2–Nd1–O7	78.16(5)	O6–Nd1–O6a	76.39(5)	O1W–Nd1–O6a	103.67(4)
O6–Nd1–O7	146.53(5)	O3–Nd1–O6a	71.53(4)	O9–Nd1–O8	52.38(5)

modes [28–30]. The absence of the characteristic bands around 1700 cm^{-1} shows that the Hcbba ligands are completely deprotonated in the form of $cbba^-$ anions upon reaction with the metal ions [31,32]. The same conclusions are also supported by the results obtained from X-ray diffraction measurements.

Table 3
Hydrogen-bond lengths (Å) and angles (°) for coordination polymers **I**–**III**.

D–H···A	d(D–H)	d(H···A)	d(D···A)	∠(DHA)
I				
C19–H19···Cl3	0.93	3.11	3.77	130.0
O1W–H1WA···O7	0.85	2.07	2.85	152.9
O1W–H1WB···O5	0.85	2.32	2.85	121.2
II				
C29–H29···Cl2	0.93	3.19	3.80	130.4
O1W–H1WB···O4	0.85	2.05	2.84	154.3
III				
C33–H33···Cl1	0.93	3.09	3.76	131.3
O1W–H1WB···O1	0.85	2.02	2.85	168.4

3.2. Structural description of the coordination polymers $[Ln(cbba)_3(H_2O)]_\infty$

The single-crystal analyses reveal that **I**–**III** are isomorphous and isostructural, crystallizing in monoclinic space group *C*2/*c*. Here, coordination polymer **I**, $[La(cbba)_3(H_2O)]_\infty$, is selected as an example to describe the formation of 3D structure in detail. The coordination environment of La(III) centers in coordination polymer **I** is shown in Fig. 1a, where lanthanum entity is connected with carboxylic oxygen and carbonyl atoms. Namely, La1 is nine-coordinated with the O_9 donor set containing eight oxygen atoms

Table 4
C–H···π distances (Å) for coordination polymers **I**–**III**.

I		II		III	
C38–H38···π	2.784	C24–H24···π	2.773	C10–H10···π	2.780
C23–H23···π	3.455	C37–H37···π	3.455	C37–H37···π	3.496

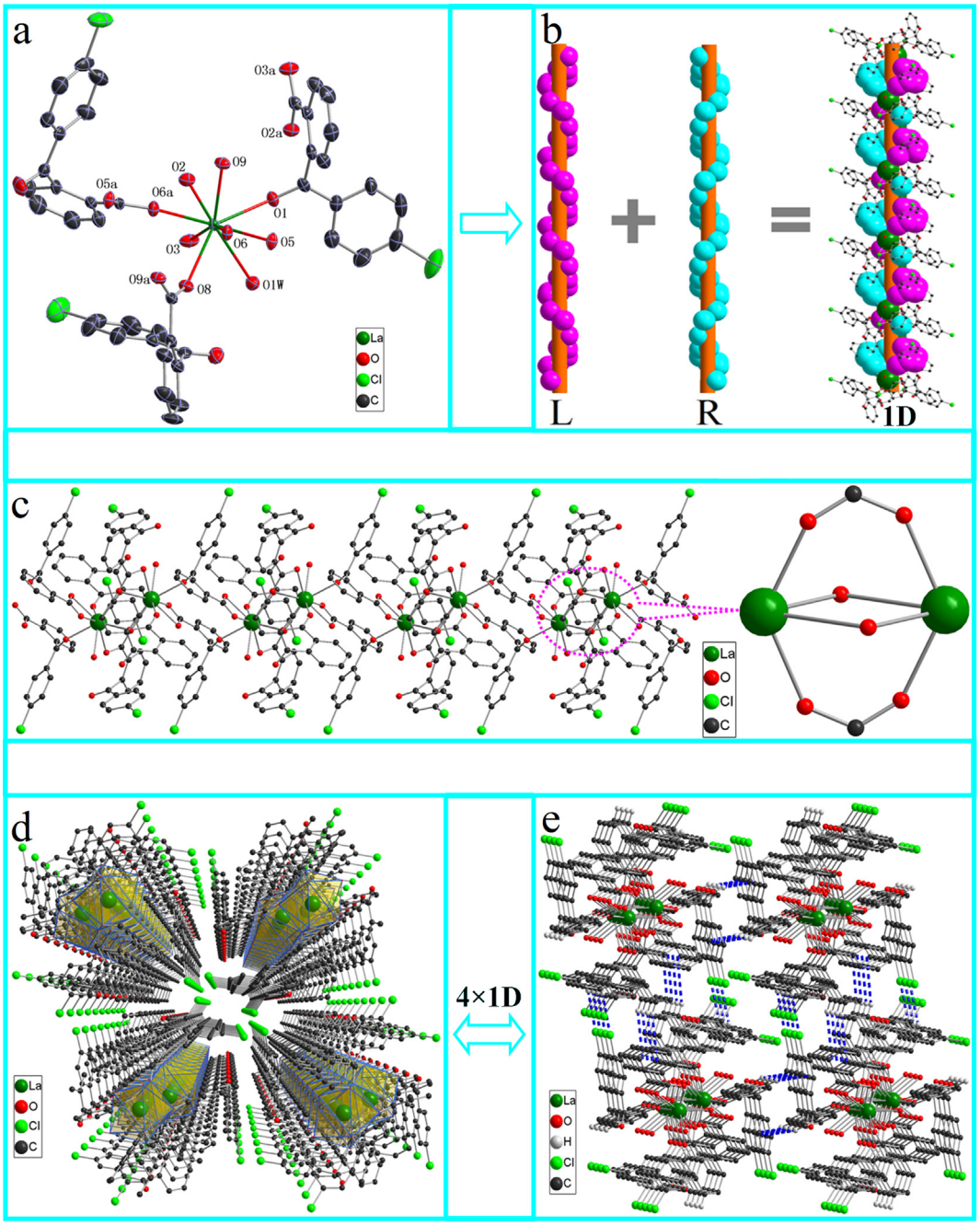

Fig. 1. (a) Diagram showing the coordination environment for La(III) centers in **I** (30% probability displacement ellipsoids); (b) Schematic representation of the double-stranded helices in 1D chain of **I** (entangled by one left-handed and one right-handed helical chain in coaxial manner); (c) Diagram showing the 1D chain of coordination polymer **I** (insert a cavate 10-membered cage ($La_2O_2(OCO)_2$)); (d) Diagram showing the 3D architecture of **I**; (e) C–Cl···H and C–H···π interactions in the 3D frameworks of **I**.

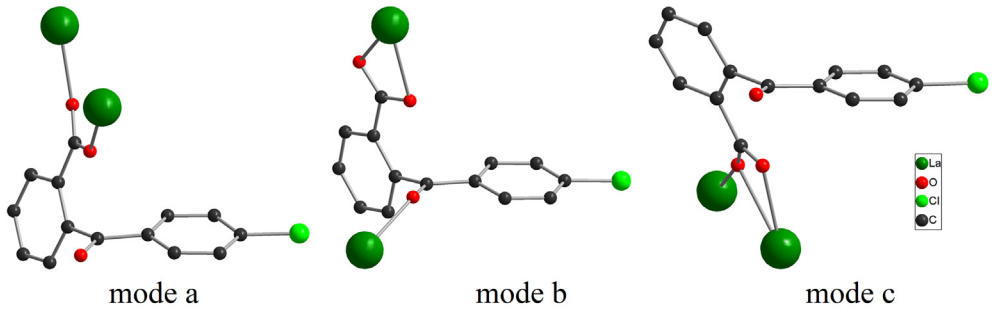

Scheme 1. Coordination modes of $cbba^-$ ligand in coordination polymers **I**–**III**.

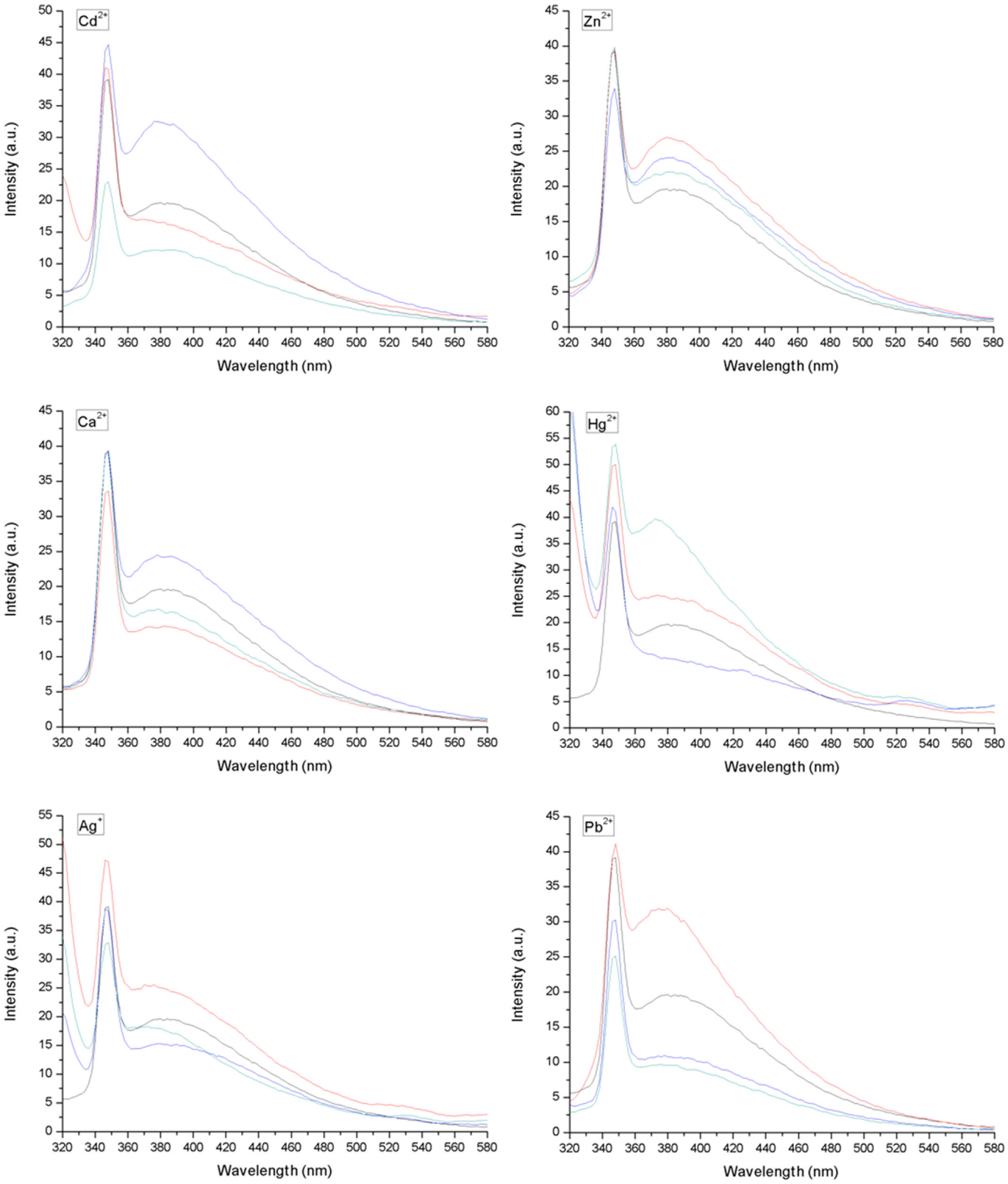

Fig. 2. Luminescent intensity of **II** at 349 nm and 379 nm in water at room temperature upon the addition of Cd^{2+}, Zn^{2+}, Ca^{2+}, Hg^{2+}, Ag^{+} and Pb^{2+} ions (excited at 309 nm)(black, no addition; red, 10^{-4} M; blue, 2×10^{-4} M; green, 3×10^{-4} M). (For interpretation of the references to colour in this figure legend, the reader is referred to the web version of this article.)

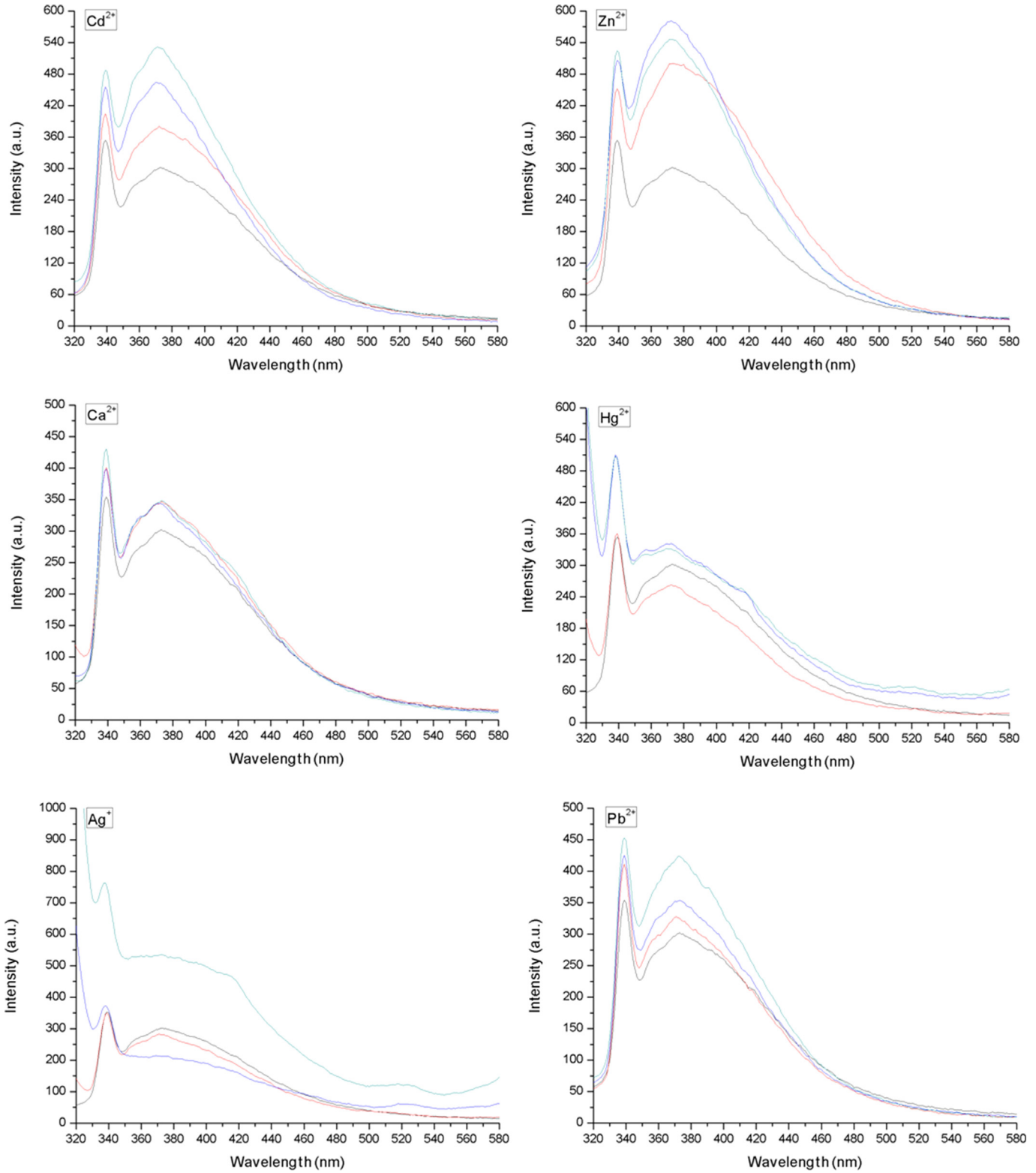

Fig. 3. Luminescent intensity of **III** at 347 nm and 368 nm in water at room temperature upon the addition of Cd^{2+}, Zn^{2+}, Ca^{2+}, Hg^{2+}, Ag^{+} and Pb^{2+} ions (excited at 302 nm)(black, no addition; red, 10^{-4} M; blue, 2×10^{-4} M; green, 3×10^{-4} M). (For interpretation of the references to colour in this figure legend, the reader is referred to the web version of this article.)

coming from six $cbba^{-}$ anions (O1, O2, O3, O5, O6, O6a, O8, O9) and one molecule of terminal water (O1W). Besides, La1 ion in the asymmetric coordination unit of **I** presents distorted tricapped trigonal prism configurations, and three kinds of coordination modes *a*, *b* and *c* exist in the structure (as illustrated in Scheme 1), in which two $cbba^{-}$ anions adopt bidentate *a* mode (in μ_2-η^1:η^1 fashion), two adopt tridentate *b* mode (in μ_2-η^1:η^1:η^1 fashion), and two adopt tridentate *c* mode (in μ_2-η^1:η^2 fashion), respectively. The

La–O_{cbba} distances range from 2.426(3)–2.872(3) Å (La1–O9 = 2.426(3), La1–O2 = 2.558(3), La1–O3 = 2.527(3), La1–O6 = 2.465(3), La1–O5 = 2.534(3), and La1–O8 = 2.471(3) Å, respectively), and those of La–$O_{carbonyl}$ (La1–O1) and La–O_W (La1–OW)are 2.562(3) and 2.660(4) Å, respectively. The average bond length of La–$O_{carboxyl}$ is 2.532 Å which is significantly shorter than those of La–O_W and La–$O_{carbonyl}$. The ∠O–La–O bond angles are in the range of 47.69(10)–146.20(11)°. The data of bond lengths and bond angles in the present work are consistent with those in previous work covering lanthanide coordination polymers [33–35].

The adjacent two crystallographically equivalent La(III) ions (La···La) are bridged by two oxygen atoms (i.e. O6 and O6a) and two carboxy groups (i.e. O8a–C42–O9) and (O8–C42–O9a) in μ_2-η^1:η^1 fashion with the nonbonding distance of 4.220 Å to form a cavate 10-membered cage ($La_2O_2(OCO)_2$) which acts as the subunit in the 3D architecture (see Fig. 1c). In terms of the framework of coordination polymer **I**, every two adjacent 10-membered cages ($La_2O_2(OCO)_2$) are connected into a 1D infinite chain through two $cbba^-$ anions in μ_2-η^1:η^1 fashion (mode *b*) which are further assembled into 3D architecture (see Fig. 1d) *via* C–H···π (i.e. C23–H23···π = 3.455 Å and C38–H38···π = 2.784 Å) and C–H···Cl interactions (C19–H19···Cl3 = 3.113 Å) between the neighboring reciprocally parallel 1D chains, as illustrated in Fig. 1e [36,37]. The most fascinating structural feature of **I** is that the double-stranded helix entangled by one left-handed and one right-handed helical chain in coaxial manner is observed running along the crystallographic *c axis* in 1D infinite chain, as depicted in Fig. 1b. Furthermore, both helical chains share the same atoms (indicated in green in Fig. 1b) with a pitch of 10.148 Å. This case is rather rare even though some types of helices have previously been characterized [38–44].

3.3. Luminescent properties

The luminescent properties of **II** were studied in water (10^{-4} M) at room temperature. Emission spectra of **II** (excited at 309 nm) in the presence of Cd^{2+}, Zn^{2+}, Ca^{2+}, Hg^{2+}, Ag^+ and Pb^{2+} ions with respect to **II** are illustrated in Fig. 2. The emission intensity of **II** enhances gradually upon the addition of 3 equiv. of Hg^{2+}($HgSO_4$) with respect to **II**, and its highest peak at 379 nm is nearly twice as intense as the corresponding peak of the solution without Hg^{2+}. Oppositely, the introduction of Pb^{2+}($Pb(CH_3COO)_2$) is controlled at 3 equiv., the intensity of emission spectra at 379 nm reduces by 50% compared to that without adding. Different from the above-mentioned, the introduction of Cd^{2+}($Cd(CH_3COO)_2$), Zn^{2+}($Zn(CH_3COO)_2$), Ca^{2+}($CaCl_2$), and Ag^+($AgNO_3$) into the water solution of **II** causes only minor changes of the emission intensities.

As for **III** (Fig. 3), only Ag^+($AgNO_3$) causes obvious changes in emission spectra of **III**. Namely, the emission intensity at 347 nm and 368 (excited at 302 nm) in the presence of 3 equiv. of Ag^+ ion is more than twice as intense as that of the corresponding band of **III** without Ag^+ ion (see Fig. 4). Besides, the intensity of the emission spectrum at 368 nm (excited at 302 nm) increases with increasing Cd^{2+}($Cd(CH_3COO)_2$) concentrations (1–3 equiv.). The broad emissions at 349, 379 nm of **II** (excited at 309 nm) and 347, 368 nm of **III** (excited at 302 nm) are assigned to intraligand π* → π and π* → n transition and ligand-to-metal-charge-transfer (LMCT) [45–47]. **II** and **III** may be potential ion-selective luminescent probes for Hg^{2+} and Ag^+, respectively. The mechanism accounting for the luminescent feature of the coordination polymers along with its dependence on the co-existing metal ions is still under investigation.

Moreover, the emission spectra of coordination polymers **I**–**III** were investigated in the solid-state at room temperature (Fig. S1). Under the same excitation of 302 nm, coordination polymers **I**, **II** and **III** display quite similar characteristic emission bands in the near-infrared regions except the values of the intensities of corresponding emission bands.

4. Conclusion

In summary, three coordination polymers **I**–**III** were constructed from the flexible ligand Hcbba under hydrothermal conditions. The structural characterizations demonstrated that **I**–**III**

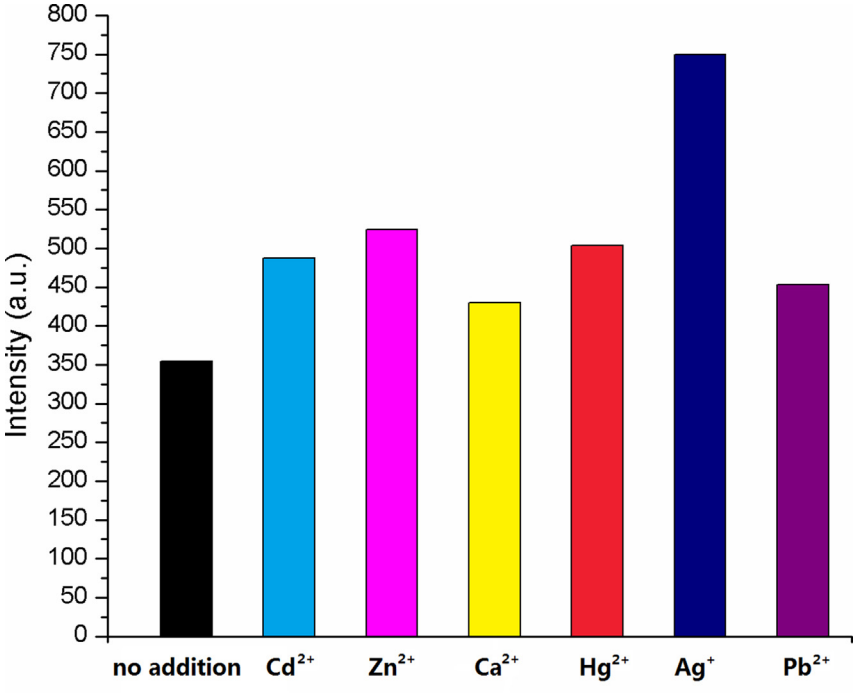

Fig. 4. Luminescent intensity of **III** at 347 nm in water at room temperature upon the addition of 3 equiv. Cd^{2+}, Zn^{2+}, Ca^{2+}, Hg^{2+}, Ag^+ and Pb^{2+} ions.

are isomorphous and isostructural, three-dimensional (3D) architecture assembled *via* C–H···π and C–H···Cl interactions between the neighboring reciprocally parallel 1D chains. In **I**–**III**, the flexible ligand Hcbba act as three types coordination modes to afford intriguing 3D frameworks. The most fascinating structural feature in **I**–**III** is that the double-stranded helices entangled by one left-handed and one right-handed helical chain in coaxial manner are observed in 1D infinite chain, and both helical chains share the same atoms. **II** and **III** may be potential ion-selective luminescent probes for Hg^{2+} and Ag^{+}, respectively.

Acknowledgments

This research is financially supported by the Natural Science Foundation of Henan Province of China (No. 13A150056, 2012B150005, 122102210174 and 12B150004).

Appendix A. Supplementary data

Supplementary data related to this article can be found at http://dx.doi.org/10.1016/j.dyepig.2014.06.010.

References

[1] Bassett AP, Magennis SW, Glover PB, Lewis DJ, Spencer N, Parsons S, et al. Highly luminescent, triple-and quadruple-stranded, dinuclear Eu, Nd, and Sm (III) lanthanide complexes based on bis-diketonate ligands. J Am Chem Soc 2004;126(30):9413–24.
[2] Wan YH, Zhang LP, Jin LP, Gao S, Lu SZ. High-dimensional architectures from the self-assembly of lanthanide ions with benzenedicarboxylates and 1,10-phenanthroline. Inorg Chem 2003;42(16):4985–94.
[3] Prasad TK, Rajasekharan MV, Costes JP. A cubic 3d–4f structure with only ferromagnetic Gd–Mn interactions. Angew Chem Int Ed 2007;46(16):2851–4.
[4] Chen WT, Fukuzumi S. Ligand-dependent ultrasonic-assistant self-assemblies and photophysical properties of lanthanide nicotinic/isonicotinic complexes. Inorg Chem 2009;48(8):3800–7.
[5] Ke F, Yuan YP, Qiu LG, Shen YH, Xie AJ, Zhu JF, et al. Facile fabrication of magnetic metal–organic framework nanocomposites for potential targeted drug delivery. J Mater Chem 2011;21(11):3843–8.
[6] Chandrasekhar V, Hossain S, Das S, Biswas S, Sutter JP. Rhombus-shaped tetranuclear [Ln_4] complexes [Ln = Dy (III) and Ho (III)]: synthesis, structure, and SMM behavior. Inorg Chem 2013;52(11):6346–53.
[7] Lee JY, Farha OK, Roberts J, Scheidt KA, Nguyen ST, Hupp JT. Metal–organic framework materials as catalysts. Chem Soc Rev 2009;38(5):1450–9.
[8] Li JR, Kuppler RJ, Zhou HC. Selective gas adsorption and separation in metal–organic frameworks. Chem Soc Rev 2009;38(5):1477–504.
[9] Ma ML, Ji C, Zang SQ. Syntheses, structures, tunable emission and white light emitting Eu^{3+} and Tb^{3+} doped lanthanide metal–organic framework materials. Dalt Trans 2013;42(29):10579–86.
[10] Wu JY, Yeh TT, Wen YS, Twu J, Lu KL. Unusual robust luminescent porous frameworks self-assembled from lanthanide ions and 2,2′-bipyridine-4,4′-dicarboxylate. Cryst Growth Des 2006;6(2):467–73.
[11] Silva P, Ananias D, Bruno SM, Valente AA, Carlos LD, Rocha J, et al. Photoluminescent metal–organic frameworks–rapid preparation, catalytic activity, and framework relationships. Eur J Inorg Chem 2013;2013(32):5576–91.
[12] Geißler D, Linden S, Liermann K, Wegner KD, Charbonnière LJ, Hildebrandt N. Lanthanides and quantum dots as förster resonance energy transfer agents for diagnostics and cellular imaging. Inorg Chem 2014;53(4):1824–38.
[13] Hołyńska M, Korabik M. Preparation and properties of a series of [Cr_2Ln_2] oximato–bridged complexes. Eur J Inorg Chem 2013;2013(31):5469–75.
[14] Perrier M, Kenouche S, Long J, Thangavel K, Larionova J, Goze-Bac C, et al. Investigation on NMR relaxivity of nano-sized cyano-bridged coordination polymers. Inorg Chem 2013;52(23):13402–14.
[15] Kanetomo T, Ishida T. Preparation and characterization of [$Gd(hfac)_3$(DTBN)(H_2O)](DTBN = di-t-butyl nitroxide). ferromagnetic Gd^{3+}–Gd^{3+} super–superexchange. Chem Commun 2014;50:2529–31.
[16] Zhao B, Chen XY, Cheng P, Liao DZ, Yan SP, Jiang ZH. Coordination polymers containing 1D channels as selective luminescent probes. J Am Chem Soc 2004;126(47):15394–5.
[17] Wang P, Ma JP, Dong YB, Huang RQ. Tunable luminescent lanthanide coordination polymers based on reversible solid-state ion-exchange monitored by ion-dependent photoinduced emission spectra. J Am Chem Soc 2007;129(35):10620–1.
[18] Allendorf MD, Bauer CA, Bhakta RK, Houk RJT. Luminescent metal–organic frameworks. Chem Soc Rev 2009;38(5):1330–2.
[19] Halim M, Tremblay MS, Jockusch S, Turro NJ, Sames D. Transposing molecular fluorescent switches into the near-IR: development of luminogenic reporter substrates for redox metabolism. J Am Chem Soc 2007;129(25):7704–5.
[20] Silva P, Cunha-Silva L, Silva NJO, Rocha J, Paz FAA. Metal–organic frameworks assembled from erbium tetramers and 2,5-pyridinedicarboxylic acid. Cryst Growth Des 2013;13(6):2607–17.
[21] Yang LR, Song S, Shao CY, Zhang HM, Zhang W, Bu ZW, et al. Synthesis, structure and luminescent properties of 3D lanthanide (La(III), Ce(III)) coordination polymers possessing 1D nanosized cavities based on pyridine-2,6-dicarboxylic acid. Synth Met 2011;161(15):1500–8.
[22] Yang LR, Song S, Shao CY, Zhang W, Zhang HM, Bu ZW, et al. Synthesis, structure and luminescent properties of two-dimensional lanthanum(III) porous coordination polymer based on pyridine-2,6-dicarboxylic acid. Synth Met 2011;161(11):925–30.
[23] Yang LR, Song S, Zhang HM, Wu LZ. Synthesis, characterization and thermal decomposition kinetics as well as evaluation of luminescent properties of several 3D lanthanide coordination polymers as selective luminescent probes of metal ions. Synth Met 2012;162(21):1775–88.
[24] Yang LR, Song S, Zhang W, Zhang HM, Bu ZW, Ren TG. Synthesis, structure and luminescent properties of neodymium(III) coordination polymers with 2,3-pyrazinedicarboxylic acid. Synth Met 2011;161(9):647–54.
[25] Raman NK. Infrared and Raman spectra of inorganic and coordination chemistry. New York: Wiley; 1997.
[26] Tang RR, Gu GL, Zhao Q. Synthesis of Eu(III) and Tb(III) complexes with novel pyridine dicarboxamide derivatives and their luminescence properties. Spectrochim Acta Part A 2008;71(2):371–6.
[27] Yang LR, Song S, Zhang W, Zhang HM, Bu ZW, Ren TG. Synthesis, structure of 3D lanthanide (La(III), Pr(III)) nanoporous coordination polymers containing 1D channels as selective luminescent probes of Pb^{2+}, Ca^{2+} and Cd^{2+} ions. Synth Met 2011;161(11):2230–40.
[28] Shi FN, Cunha-Silva L, Trindade T, Paz FAA, Rocha J. Three-dimensional lanthanide–organic frameworks based on di-, tetra-, and hexameric clusters. Cryst Growth Des 2009;9(5):2098–109.
[29] Tancrez N, Feuvrie C, Ledoux I, Zyss J, Toupet L, Le Bozec H, et al. Lanthanide complexes for second order nonlinear optics: evidence for the direct contribution of f electrons to the quadratic hyperpolarizability 1. J Am Chem Soc 2005;127(39):13474–5.
[30] Li XF, Han ZB, Cheng XN, Chen XM. Studies on the radii dependent lanthanide self-assembly coordination behaviors of a flexible dicarboxylate ligand. Inorg Chem Commun 2006;9(11):1091–5.
[31] Liu MS, Yu QY, Cai YP, Su CY, Lin XM, Zhou XX, et al. One-, two-, and three-dimensional lanthanide complexes constructed from pyridine-2,6-dicarboxylic acid and oxalic acid ligands. Cryst Growth Des 2008;8(11):4083–91.
[32] Aghabozorg H, Moghimi A, Manteghi F, Ranjbar M. A nine-coordinated ZrIV complex and a self-assembling system obtained from a proton transfer compound containing 2,6-pyridinedicarboxylate and 2,6-pyridinediammonium; synthesis and X-ray crystal structure. Z Anorg Allg Chem 2005;631(5):909–13.
[33] Dong YB, Wang P, Ma JP, Zhao XX, Wang HY, Tang B, et al. Coordination-driven nanosized lanthanide "molecular lantern" with tunable luminescent properties. J Am Chem Soc 2007;129(16):4872–3.
[34] Chen ML, Guo YC, Yang F, Liang JX, Cao ZX, Zhou ZH. A lanthanum chelate possessing an open-channel framework with water nanotubes: properties and desalination. Dalt Trans 2014. http://dx.doi.org/10.1039/c3dt52837e.
[35] Vilela SMF, Fernandes JA, Ananias D, Carlos LD, Rocha J, Tomé JPC, et al. Photoluminescent layered lanthanide–organic framework based on a novel trifluorotriphosphonate organic linker. CrystEngComm 2014;16(3):344–58.
[36] Hu YL, Li YY, Yu JY, Li JJ, Wu XX, Ye HQ, et al. Syntheses, crystal structures and magnetic properties of three new molecular magnets by self-assembly of bis(maleonitriledithiolate) nickel(III) anion and substituted N, N′-dibenzylpiperidinium. Synth Met 2013;176:31–40.
[37] Karanam M, Choudhury AR. Study of halogen-mediated weak interactions in a series of halogen-substituted azobenzenes. Cryst Growth Des 2013;13(11):4803–14.
[38] Jiang JJ, Zheng SR, Liu Y, Pan M, Wang W, Su CY. Self-assembly of triple helical and meso-helical cylindrical arrays tunable by bis-tripodal coordination converters. Inorg Chem 2008;47(22):10692–9.
[39] Ghosh SK, Bharadwaj PK. Coexistence of water dimer and hexamer clusters in 3D metal-organic framework structures of Ce(III) and Pr(III) with pyridine-2,6-dicarboxylic acid. Inorg Chem 2003;42(25):8250–4.
[40] Han L, Hong MC, Wang RH, Luo JH, Lin ZZ, Yuan DQ. A novel nonlinear optically active tubular coordination network based on two distinct homochiral helices. Chem Commun 2003;20:2580–1.
[41] Kondo M, Miyazawa M, Irie Y, Shinagawa R, Horiba T, Nakamura A, et al. A new Zn (II) coordination polymer with 4-pyridylthioacetate: assemblies of homo-chiral helices with sulfide sites. Chem Commun 2002;18:2156–7.
[42] Yang LR, Wu LZ, Liu L, Zhang HM, Li MX. Three novel transition metal coordination polymers based on (2,3-f)-pyrazino (1,10) phenanthroline-2,3-dicarboxylic acid sodium salt: hydrothermal syntheses, structures, and properties. Dye Pigment 2014;101:196–202.
[43] Zhao XQ, Zhao B, Shi W, Cheng P. Structures and luminescent properties of a series of Ln–Ag heterometallic coordination polymers. CrystEngComm 2009;11(7):1261–9.

[44] Guo F, Wang F, Yang H, Zhang X, Zhang J. Tuning structural topologies of three photoluminescent metal–organic frameworks via isomeric biphenyldicarboxylates. Inorg Chem 2012;51(18):9677–82.
[45] Xu J, Cheng J, Su W, Hong M. Effect of lanthanide contraction on crystal structures of three-dimensional lanthanide based metal–organic frameworks with thiophene-2,5-dicarboxylate and oxalate. Cryst Growth Des 2011;11(6):2294–301.
[46] Gu JZ, Kirillov AM, Wu J, Lv DY, Tang Y, Wu JC. Synthesis, structural versatility, luminescent and magnetic properties of a series of coordination polymers constructed from biphenyl-2,4,4′-tricarboxylate and different N-donor ligands. CrystEngComm 2013;15(47):10287–303.
[47] Jia H, Li Y, Xiong Z, Wang C, Li G. Five metal–organic frameworks from 3,4-dimethylphenyl substituted imidazole dicarboxylate: syntheses, structures and properties. Dalt Trans 2014;43:3704–15.